

Fig. 3 Comparison of OPM and OSA measurements around 1395 nm water absorption peak

*Acknowledgments:* D.A. Chestnut is supported by a UK Engineering and Physical Science Research Council (EPSRC) studentship.

© IEE 2003

16 June 2003

Electronics Letters Online No: 20030790

DOI: 10.1049/el:20030790

D.A. Chestnut and J.R. Taylor (*Femtosecond Optics Group, Physics Department, Imperial College London, Prince Consort Road, London SW7 2BW, United Kingdom*)

E-mail: david.chestnut@imperial.ac.uk

#### References

- 1 POPOV, S.V., CHERNIKOV, S.V., and TAYLOR, J.R.: '6-W average power green light generation using seeded high power ytterbium fibre amplifier and periodically poled KTP', *Opt. Commun.*, 2000, **174**, pp. 231–234
- 2 KAWAL, H., TOKUHISA, A., DOI, M., MIWA, S., MATSUURA, H., KITANO, H., and OWA, S.: 'UV light source using fiber amplifier and nonlinear wavelength conversion' in 'OSA Trends in Optics and Photonics (TOPS), Conference on Lasers and Electro-Optics'. OSA Technical Digest, Postconference Edition (Optical Society of America, Washington, DC, 2003), cTuT4
- 3 GRUBB, S.G.: '1.3  $\mu\text{m}$  cascaded raman amplifiers' in 'Optical amplifiers and their applications', Vol. 18, 1995, OSA Technical Digest Series (Optical Society of America, Washington, DC, 1995), pp. SaA1-1–SaA1-3
- 4 PUC, A.B., CHBAT, M.W., HENRIE, J.D., WEAVER, N.A., KIM, H., KAMINSKI, A., RAHMAN, A., and FÉVRIER, H.A.: 'Long-haul WDM NRZ transmission at 10.7 Gb/s in S-band using cascade of lumped Raman amplifiers' in 'OSA Trends in Optics and Photonics (TOPS), Vol. 54, Optical Fiber Communication Conference'. Technical Digest, Postconference Edition (Optical Society of America, Washington, DC, 2001), pp. PD39-1–PD39-3
- 5 REEVES-HALL, P.C., CHESTNUT, D.A., DE MATOS, C.J.S., and TAYLOR, J.R.: 'Dual wavelength pumped L- and U-band Raman amplifier', *Electron. Lett.*, 2001, **37**, p. 883
- 6 MIYA, T., TERUNUMA, Y., HOSAKA, T., and MIYASHITA, T.: 'Ultimate low-loss single-mode fibre at 1.55  $\mu\text{m}$ ', *Electron. Lett.*, 1979, **15**, pp. 106–108

## High-performance 40 Gbit/s fibre Bragg grating tunable dispersion compensator fabricated using group delay ripple correction technique

M. Sumetsky, N.M. Litchinitser, P.S. Westbrook, P.I. Reyes, B.J. Eggleton, Y. Li, R. Deshmukh, C. Soccolich, F. Rosca, J. Bennike, F. Liu and S. Dey

A recently proposed UV correction method is used to reduce group delay ripple in a chirped fibre grating tunable dispersion compensator. In 43 Gbit/s CSRZ system tests, the corrected grating had less than 0.5 dB OSNR penalty over the tunable dispersion range of 270 to 750 ps/nm.

Group delay ripple (GDR) is one of the most significant impediments in the application of chirped fibre Bragg gratings (CFBG) for dispersion compensation. GDR is defined as the deviation from the desired linear group delay against wavelength and gives rise to substantial OSNR penalty [1, 2]. It originates from both random and systematic errors introduced during the fibre grating fabrication process. For a tunable DC FBG, the tuning mechanism can also introduce small variations in GD. Several papers suggested different modifications of the fibre grating fabrication process in order to reduce GDR [3–6]. It is known that the high-frequency GDR components (e.g. for 43 Gbit/s, having a period  $<0.1$  nm in wavelength) do not significantly contribute to the OSNR penalty [2, 7] and experience a fundamental high-frequency cutoff [8]. Recently, a method for low-frequency GDR correction by successive UV exposures was suggested [9]. This method enables trimming of both systematic and random components of GDR and is an effective tool for fabrication of high-performance dispersion compensation devices. In this Letter we report the fabrication of a low GDR tunable dispersion compensator (TDC) using the technique developed in [9].

Our technique is based on iterative correction of the GDR. To correct slowly varying GDR we used an approximate 'adiabatic' solution of the inverse problem relating GDR against wavelength to UV correction exposure against position. Because the correction is iterative, it does not fully rely on the accuracy of this solution and is equally well suited for the improvement of systematic and random components of the GDR, unlike the approach of [6]. Below we describe the principles of UV correction of CFBGs and demonstrate a TDC that was fabricated using our new technique. The low-frequency GDR of the grating used in the TDC is corrected from  $\pm 10$  to  $\pm 2$  ps. The OSNR penalty measured for 43 Gbit/s CSRZ signal transmission is  $<0.5$  dB for the entire tuning dispersion range of 270 to 750 ps/nm, and carrier frequencies in the detuning range of  $\pm 10$  GHz. The value of the measured OSNR penalty is in good agreement with the one obtained by numerical simulation, which indicated reduction of OSNR penalty after GDR correction from 4 dB to  $<1$  dB.

Our method of GDR correction is shown in Fig. 1. First, the grating is inscribed using the conventional phase mask UV grating writing technique (Fig. 1a). Immediately after the CFBG is written its GDR is characterised (Fig. 1b). Then, by an approximate adiabatic treatment of the group delay, discussed further below, we determine the required index profile to reduce the measured GDR (Fig. 1c). Lastly, this index variation is introduced by direct 'DC' UV exposure (Fig. 1d). We continue the iterative steps (b  $\rightarrow$  c  $\rightarrow$  d  $\rightarrow$  b) of the UV trimming until the desired reduction of the GDR is achieved.

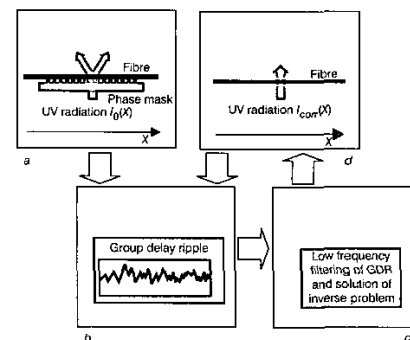


Fig. 1 Scheme of fibre grating correction

a Fibre grating writing c Determination of correction index  
b Characterisation d Correction

We assume that the GDR is relatively small (usually it is  $\sim 10$  ps for dispersion  $\sim 1000$  ps/nm and reflection bandwidth  $\sim 1$  nm) and slowly varying (we are correcting the low-frequency part of the GDR). Then, in the simplest adiabatic approximation, the DC index variation,  $\delta n_{DC}(x)$  which compensates the GDR,  $\delta\tau(\lambda)$ , is defined by

$$\delta n_{DC}(x) = \text{const} \frac{c n_{eff} C_{gr}}{2\Lambda_{gr}} \delta\tau(2n_{eff} C_{gr} x) \quad (1)$$

where  $c$  is the speed of light in vacuum,  $n_{eff}$  is the effective index,  $C_{gr} = d\Lambda_{gr}/dx$  is the chirp rate of the grating period, and  $const$  is of order 1 and is determined by experimental calibration. Eqn. (1) shows that in the adiabatic approximation the compensating DC index is simply determined by rescaling the plot of GDR. It follows from (1) that  $\delta n_{DC}(x)$  which compensates GDR with amplitude 10 ps is  $\sim 10^{-5}$ . Here we consider strong gratings when the reflection amplitude is very close to unity and the reflection amplitude ripple introduced by  $\delta n_{DC}(x)$  is negligible.

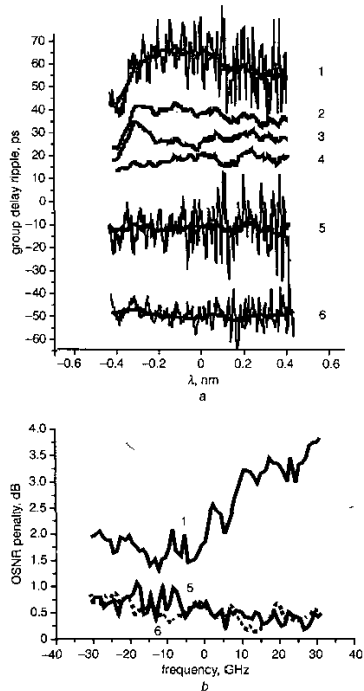


**Fig. 2** Iterative process of grating correction, and simulated OSNR penalties

*a* Iterative process of grating correction: GDR (thin line) and GDR averaged over 0.1 nm (bold line) after several correction steps, from 1 (initial) to 5 (final). Curves 6 show GDR and averaged GDR of grating after grating anneal  
*b* Simulated OSNR penalties for original (1), corrected (5, solid curve) and annealed (6, dotted curve) gratings

In our application, we consider a CFBG with a grating period  $\Lambda_{gr} = 548$  nm, chirp  $C = 0.048$  nm/cm, grating length 10 cm, and amplitude of index modulation  $\sim 3 \cdot 10^{-4}$ . The dispersion of the CFBGs is around 780 ps/nm and the GDR is  $\sim \pm 20$  ps. For these grating parameters, (1) is reasonably accurate if the spatial resolution of index variation is  $\geq 1$  cm and, respectively, the characteristic wavelength of GDR variation is  $\geq 0.1$  nm. At 43 Gbit/s GDR with variation on this wavelength scale is the major contribution to OSNR penalty [2], therefore the adiabatic approximation of (1) is sufficient to compute the UV correction exposures. In general, for larger dispersions and smaller bit rates a more complete inverse algorithm is required [9].

Fig. 2a shows the original GDR of the grating considered, and the result of its averaging over 0.1 nm. The correction of the averaged GDR was performed in several iterations by successive elimination of individual ripples. Fig. 2a shows the results of several steps of correction. It demonstrates reduction of averaged GDR from  $\pm 10$  ps to  $\pm 2$  ps.

Fig. 2b demonstrates the corresponding dramatic improvement in CFBG performance obtained numerically when these devices are implemented in a 43 Gbit/s CSRZ transmission simulation. In our numerical simulations we model CFBG as a linear filter. This filter is fully characterised by its amplitude and phase against wavelength. To calculate transmission penalty we first make a linear fit to the measured group delay over the high-reflection bandwidth of the grating and subtract this linear fit from the original group delay. We calculate numerically the corresponding eye-opening penalty (EOP) and then use

an approximate relationship for OSNR penalty [in dB]  $\approx 2 \times \text{EOP}$  [in dB] [10]. In our simulations, we send a CSRZ pulse sequence through the device under test, which is determined by its amplitude ripple and GDR, and calculate the EOP after transmission through an ideal photodiode having 1 A/W responsivity (no thermal noise, dark current, and shot noise) and a fifth-order electrical Bessel filter.

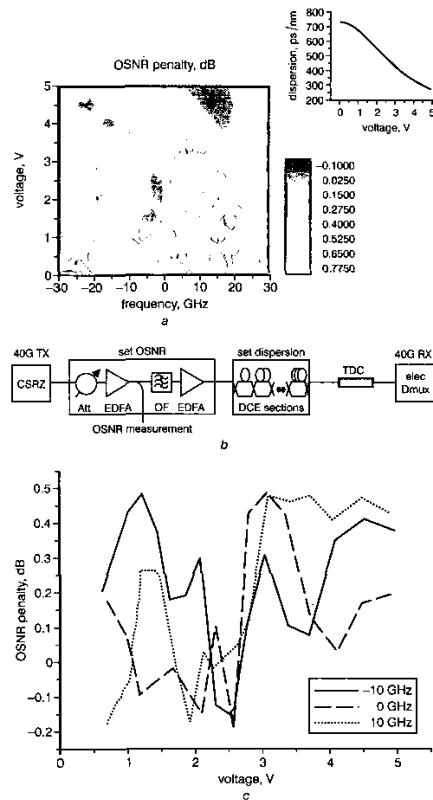


**Fig. 3** OSNR penalty

*a* OSNR penalty calculated for TDC device fabricated from annealed grating of Fig. 2b, curves 3, against voltage and carrier frequency for 43 Gbit/s CSRZ  
Inset: Introduced dispersion against applied voltage  
*b* Experimental setup for OSNR measurement (Att: attenuator; OF: optical filter; DCF: dispersion compensating fibre)  
*c* OSNR penalty for same device for -10, 0, 10 GHz carrier frequency shifts

The OSNR penalty is reduced from 4 dB to  $< 1$  dB in a  $\pm 30$  GHz bandwidth of carrier frequencies. Note that our results highlight the dominant contribution of the low-frequency GDR to OSNR penalty, since the high-frequency ripple is about the same after grating correction.

After annealing of the corrected grating (for thermal stabilisation), its reflectivity was reduced from 99.995% to  $\sim 90\%$ . The high-frequency component of its GDR was also reduced by roughly a factor of 3, while the low-frequency GDR remained and the OSNR penalty was approximately unchanged (see Figs. 2a and b curves 6). A TDC device was fabricated by integrating a resistive thin-film heater in close thermal contact with the fibre grating [2]. The dispersion of the TDC was tuned by the voltage applied to the film, which changed its temperature [2]. Fig. 3a shows the results of OSNR penalty calculated for the fabricated TDC. These simulations show that the OSNR penalty was  $< 0.8$  dB for carrier frequency variation of  $\pm 30$  GHz and dispersion variation between 750 and 270 ps/nm. The OSNR penalty was also measured experimentally using the setup shown in Fig. 3b. The 43 Gbit/s CSRZ signal was controlled by adjusting the input power into an EDFA. The dispersion was varied by sending the signal through various lengths of DCF. The TDC was inserted in front of an ETDM receiver. Fig. 3c shows the result of OSNR penalty measurement for carrier frequency shifts of -10, 0 and 10 GHz against applied voltage. This carrier frequency deviation accounts for possible drift of the laser and grating

central frequency. The measured OSNR penalties did not exceed 0.5 dB and were in reasonable agreement with numerical simulations.

© IEE 2003

29 May 2003

Electronics Letters Online No: 20030716

DOI: 10.1049/el:20030716

M. Sumetsky, N.M. Litchinitser, P.S. Westbrook and P.I. Reyes (OFS Laboratories, 600 Mountain Ave., Murray Hill, NJ 07974, USA)

B.J. Eggleton (CUDOS—Center for Ultra-high bandwidth Devices for Optical Systems, School of Physics, University of Sydney, NSW 2006, Australia)

Y. Li, R. Deshmukh and C. Soccolich (Specialty Photonic Devices, OFS, 19 Schoolhouse Road, Somerset, NJ 08873, USA)

F. Rosca, J. Bennike, F. Liu and S. Dey (Mintera Corporation, 847 Rogers St., Lowell, MA 01852, USA)

## References

- 1 KASHYAR R.: 'Fiber Bragg gratings' (Academic Press, 1999)
- 2 EGGLETON, B.J., *et al.*: 'Integrated tunable fiber gratings for dispersion management in high-bit rate systems', *J. Lightwave Technol.*, 2000, **18**, pp. 1418–1432
- 3 RIANI, I., *et al.*: 'Chirped fiber Bragg gratings for WDM chromatic dispersion compensation in multispan 10-Gb/s transmission', *IEEE J. Sel. Top. Quantum Electron.*, 1999, **5**, pp. 1312–1324
- 4 MIHAILOV, S.J., *et al.*: 'Apodization technique for fiber grating fabrication with a half-tone transmission amplitude mask', *Appl. Opt.*, 2000, **39**, pp. 3670–3677
- 5 KOMUKAI, T., INUI, T., and NAKAZAWA, M.: 'Very low group delay ripple characteristics of fibre Bragg grating with chirp induced by an S-curve bending technique', *Electron. Lett.*, 2001, **37**, pp. 449–451
- 6 BURYAK, A.V., and STEPANOV, D.YU.: 'Correction of systematic errors in the fabrication of fiber Bragg gratings', *Opt. Lett.*, 2002, **27**, pp. 1099–1101
- 7 ENNSER, K., *et al.*: 'Influence of nonideal chirped fiber grating characteristics on dispersion cancellation', *IEEE Photonics Technol. Lett.*, 1998, **10**, pp. 1476–1478
- 8 SUMETSKY, M., EGGLETON, B.J., and DE STERKE, C.M.: 'Theory of group delay ripple generated by chirped fiber gratings', *Opt. Express*, 2002, **10**, pp. 332–340
- 9 SUMETSKY, M., *et al.*: 'Group delay ripple correction in chirped fiber Bragg gratings', *Opt. Lett.*, 2003, **28**, pp. 777–779
- 10 RASMUSSEN, C.J., *et al.*: 'Theoretical and experimental studies of the influence of the number of crosstalk signals on the penalty caused by incoherent optical crosstalk'. OFC 1999, San Diego, CA, USA, Paper TuR5

## Online measuring dispersion sign in optical communication systems

M. Zaacks, U. Mahlab, M. Horowitz and S. Stepanov

A new method for an online measurement of the dispersion sign in optical communication systems is demonstrated. The measurement of the dispersion sign is based on a low frequency amplitude and wavelength modulation of a DFB laser source in the transmitter. By comparing, at the receiver, the phase of the extracted clock signal to the phase of a signal, obtained due to the amplitude modulation of the DFB laser, the sign of the dispersion is determined. The new monitoring technique might be important in high data rate optical communication systems where the allowable residual dispersion is close to zero.

Online monitoring and dynamic compensation of dispersion become essential in high data rate optical communication systems ( $\geq 40$  Gbit/s). In such systems, the margin of the overall system dispersion is extremely small. Since the dispersion changes in time due to the variation of environmental conditions such as temperature or stress, online monitoring of dispersion is required. The online measurement of the dispersion should be performed without affecting the performance of the transmission system. Several methods of online dispersion measurement in optical communication systems have been demonstrated [1–6]. These measurement techniques can be used to obtain the absolute value of the dispersion, or to detect when a zero dispersion is obtained. However, the sign of the dispersion coefficient was not measured. Therefore, feedback techniques that use such monitoring

methods in dynamic dispersion compensation may not work well, especially when the desired residual dispersion is close to zero. Moreover, when a small residual dispersion is needed, it might be impossible to discriminate between a positive and a negative dispersion coefficient. In dynamic and reconfigurable networks the measurement of the dispersion sign might be required to quickly compensate for changes in the link dispersion.

In this Letter we demonstrate experimentally a new method to online monitor the sign of the dispersion in optical communication systems. The measurement technique is based on a low-frequency modulation of the power and the wavelength of a DFB laser by modulating the laser current. This current modulation changes both the carrier frequency and the power of the DFB laser, and hence the power and the wavelength modulation of the laser are synchronised and are in phase. The principle of our sign monitoring technique is based on this effect. The output of the laser is then modulated with a high data rate signal using an external modulator. The monitoring of the dispersion is carried out at the receiving end. Owing to dispersion effect, the low frequency wavelength modulation induces phase changes in the received optical clock. The amplitude of the dispersion coefficient is obtained by measuring the amplitude of these phase changes using a phase-locked loop (PLL), as described in [2]. The sign of the dispersion is obtained by comparing the phase of the periodic signal at the output of the PLL filter with the phase of the low-frequency modulation of the carrier wavelength. This wavelength modulation is directly connected to a readily-detectable amplitude modulation (AM) signal at the receiver output, caused by the low-frequency modulation of the DFB laser in the transmitter. The relative phase between the detected AM signal and the PLL error signal can be used to obtain the sign of the dispersion. The measurement of the dispersion sign and amplitude is simple and was performed without significantly affecting the system performance even when the link contained four amplifiers and fibres with a total length of up to 300 km.

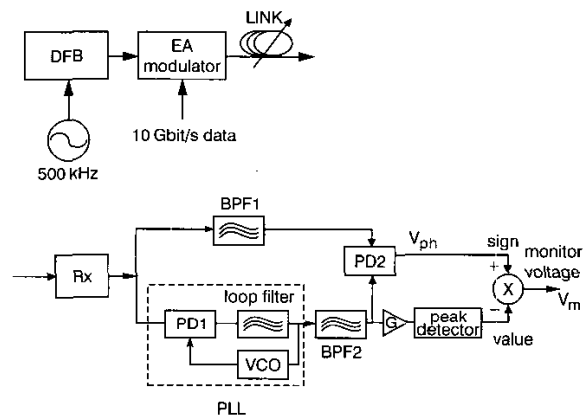


Fig. 1 Schematic description of experimental setup used to measure dispersion sign

The current of a DFB laser is periodically changed at frequency of about 500 kHz to modulate carrier frequency and amplitude of laser. The error voltage of a PLL, used to extract clock of optical signal, is compared at the receiver to a signal obtained due to amplitude modulation of laser

G: electrical amplifier; BPF1, BPF2: bandpass filters with central frequency about 500 kHz; VCO: voltage control oscillator; Rx: optical receiver; PD1, PD2: phase detectors; LINK: transmission link that includes fibres with different lengths and dispersion coefficients and up to four optical amplifiers, used to overcome loss

Fig. 1 shows a schematic description of the experimental setup. The DFB laser current was modulated with a small sinusoidal signal at a low frequency,  $\omega_l/2\pi \approx 500$  kHz. When the modulation amplitude is small and the modulation frequency is significantly smaller than the relaxation oscillation frequency of the DFB laser, the intensity and the wavelength of the laser are sinusoidally modulated with the same frequency and phase as the laser current [7]. In our experiment the peak-to-peak modulation amplitude of the current, relative power, and wavelength of the laser were 5 mA, 10.7%, and 8.7 pm, respectively. The information was added to the system at a bit rate of 10 Gbit/s by modulating the laser output using an electroabsorption modulator. At the receiver, the slow amplitude modulation of the laser was extracted using a